

Utilizing Adversarial Examples for Bias Mitigation and Accuracy Enhancement

Pushkar Shukla^{*1}, Dhruv Srikanth^{*2}, Lee Cohen³, and Matthew Turk¹

¹ Toyota Technological Institute at Chicago

² Carnegie Mellon University

³ Stanford University

{pushkarshukla,mturk}@ttic.edu,dhruvsrikanth5@gmail.com,leecohencs@gmail.com

Abstract. We propose a novel approach to mitigate biases in computer vision models by utilizing counterfactual generation and fine-tuning. While counterfactuals have been used to analyze and address biases in DNN models, the counterfactuals themselves are often generated from biased generative models, which can introduce additional biases or spurious correlations. To address this issue, we propose using adversarial images, that is images that deceive a deep neural network but not humans, as counterfactuals for fair model training. Our approach leverages a curriculum learning framework combined with a fine-grained adversarial loss to fine-tune the model using adversarial examples. By incorporating adversarial images into the training data, we aim to prevent biases from propagating through the pipeline. We validate our approach through both qualitative and quantitative assessments, demonstrating improved bias mitigation and accuracy compared to existing methods. Qualitatively, our results indicate that post-training, the decisions made by the model are less dependent on the sensitive attribute and our model better disentangles the relationship between sensitive attributes and classification variables.

Keywords: Fairness, Bias Mitigation, Responsible AI, Counterfactuals, Adversarial Examples, Curriculum Learning

1 Introduction

Computer vision systems trained on large amounts of data have been at the heart of recent technological innovation and growth. Such systems continue to find increasing use-cases in different areas such as healthcare, security, autonomous driving, remote sensing and education. However, in spite of the tremendous promise of large vision models, several studies have demonstrated the presence of unwanted societal biases in these models [6, 7, 18]. Therefore, understanding and mitigating these biases is crucial for deploying such applications in real-world scenarios.

Several approaches have been proposed to mitigate [7, 18, 22, 30, 37, 46, 54, 55, 59], measure [3, 12], and explain [2, 13, 61] biases in computer vision models. Among these approaches, the use of counterfactuals has emerged as a promising

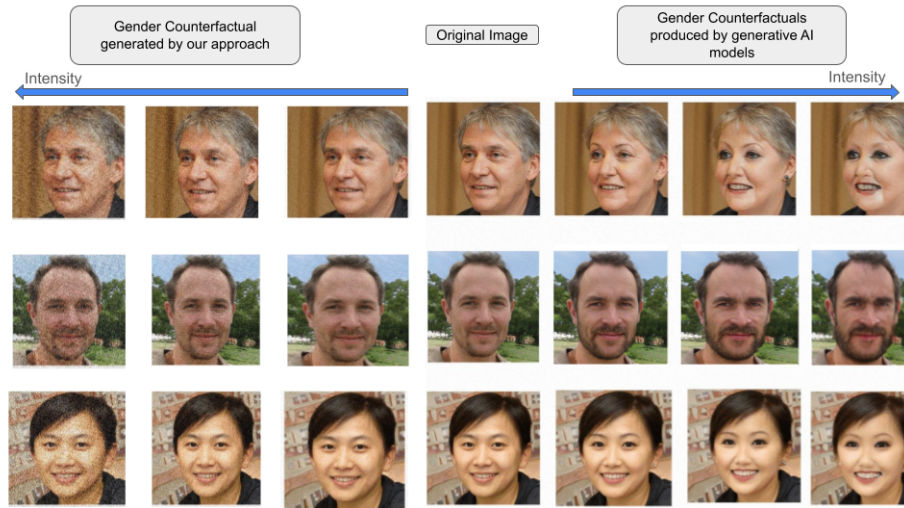


Fig. 1: An example of gender counterfactuals produced by StyleGAN2 versus our method, for a smile classification task. StyleGAN2’s images (right) correlate femininity with darker lipstick and exaggerated smiling, introducing biases. Our approach (left) generates ASACs that retain the same visual appearance as the original image.

and prominent line of research [2, 3, 12, 13, 61]. A counterfactual for an image, within the context of a model, is a modified version of the original image where certain regions are systematically replaced. This alteration is used to assess the output of the system when presented with the modified image, while ensuring that the modified image remains similar to the original in terms of its key features and characteristics [53].

However, current counterfactual generation algorithms used for bias mitigation have several limitations. Firstly, most of these algorithms rely on generative models to produce image counterfactuals with respect to a sensitive attribute (e.g., race, gender). Counterfactuals generated by these image generation mechanisms may inherently contain spurious correlations due to the presence of bias in the image generation model.

One such example of biased counterfactuals produced by an image generation model, StyleGAN2 [24], is illustrated for smile classification in Figure 1, where female counterfactuals generated by the model exhibit exaggerated smiles and dark makeup. Using such counterfactuals to address gender biases in smile prediction may exacerbate the issue they were meant to solve. Additionally, generating counterfactuals based on sensitive attributes like race or gender raises ethical concerns regarding the stereotypes associated with images generated along dimensions of a sensitive attribute. For instance, attributing specific appearances (heavy makeup and increased smile) to female faces may oversimplify their diversity. Therefore, to ensure fairness in computer vision models, we must carefully

generate and integrate counterfactuals without introducing new or exacerbating already present biases.

In this paper, we propose the use of adversarial images as an alternative approach to generative models for constructing image counterfactuals in the context of assessing and mitigating biases in computer vision models. While adversarial images have traditionally been designed to deceive computer vision models, our work advocates for their application as counterfactuals, as a way to improve computer vision models, in fairness metrics as well as accuracy. We introduce a method that leverages existing adversarial techniques to construct counterfactuals that deceive a vision model along the dimensions of sensitive attributes. We refer to these examples as ‘‘Attribute-Specific Adversarial Counterfactuals’’ or ASACs. Our method ensures that ASACs retain the visual appearance of the original image, effectively addressing ethical concerns regarding the quality of image counterfactuals. By keeping parts of the image unaltered, the likelihood of introducing spurious correlations (propagated by the generative model during the image generation process) into the fairness mitigation pipeline is markedly reduced.

Additionally, our work introduces a novel curriculum learning based fine-tuning approach that utilizes these counterfactuals to mitigate biases in vision models. Our approach looks at ASACs generated at different noise magnitudes and assigns a learning curriculum to these examples based on their ability to fool the model. We then fine-tune an already biased model using the aforementioned methodology. We validate our approach both qualitatively and quantitatively using experiments on various classifiers trained on the CelebA [31] and LFW [19] datasets. Our findings suggest that the proposed training approach, not only improves fairness metrics but also maintains or increases the overall performance of the model.

Our contributions can be summarized as follows:

- We present a bias-averse approach to generating image counterfactuals, utilizing adversarial images to create ASACs specific to sensitive attributes.
- We introduce a novel curriculum learning-based fine-tuning methodology that leverages ASACs to mitigate pre-existing biases in vision models.
- We present a comprehensive evaluation across different datasets and evaluation metrics, demonstrating that our method improves fairness metrics without compromising the overall performance of the model.

2 Related Works

Adversarial examples Adversarial examples have emerged as a notable challenge in the realm of computer vision [36, 50, 57]. These examples are crafted with the specific goal of deceiving machine learning models by making subtle alterations to input data, resulting in model misclassification. Adversarial attacks are specialized algorithms designed to generate such examples and have been the subject of extensive research. These attacks are categorized into black-box [20, 39, 43] and white-box attacks [36, 50], depending on the attacker’s access

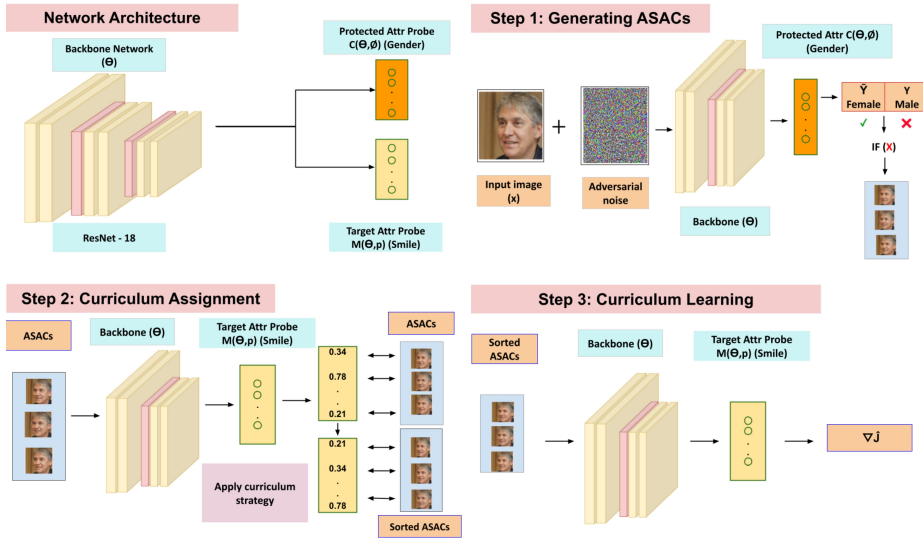


Fig. 2: Bias Mitigation Strategy: Our proposed solution for mitigating biases in a model (e.g., smile classifier) $M(\theta, \rho)$ involves training sensitive attribute classifier $C(\theta, \phi)$ (shown in the network architecture). We then follow a three-stage pipeline. (1) We generate ASACs that are able to fool $C(\theta, \phi)$. (2) We propose a curriculum assignment strategy that organizes these ASACs on their ability to fool the original model $M(\theta, \rho)$. (3) We fine-tune the original model $M(\theta, \rho)$ using ASACs and the proposed loss function (see Equation 5).

to model parameters. Our approach uses two white-box methods, FGSM [14] and PGD [34].

Bias mitigation in computer vision Bias mitigation strategies in computer vision models can be categorized into three main approaches depending on when they are deployed into the machine learning pipeline: pre-processing, in-processing, and post-processing approaches. Pre-processing methods [42, 44, 63] focus on addressing biases before training the models. This is achieved by either adjusting the data distribution or strategically augmenting existing data. In-processing techniques [45, 47, 62] try to improve the model during the training phase either by proposing an alternate training strategy or by changing the model structure. Post-processing strategies [32, 60] adjust fairness criteria after the model is trained. Our approach falls within the post-processing category as it is a method to fine-tune an already existing model concerning a protected attribute.

Counterfactuals and their role in machine learning The notion of using counterfactuals in machine learning models is closely related to the definition of counterfactual fairness proposed by Kusner et al. [28]. Counterfactuals have emerged as a versatile tool in machine learning [25, 38, 48], natural language

processing [8, 26], and computer vision [1–3, 9, 11–13, 59, 61, 63]. Counterfactual images have been used to explain [2, 13, 61], analyze [1, 3, 10, 12] and improve fairness [9, 11] in computer vision models.

The Relationship Between Counterfactual and Adversarial Examples

While the connection between counterfactuals and adversarial images has been extensively explored in theoretical machine learning [5, 23, 40, 51, 52], limited attention has been given to this relationship in computer vision [29, 41, 56, 63]. Among these approaches, the work done by Wang et al. [59] and Zhang et al. [63] is particularly noteworthy because of its proximity to our approach. Wang et al. have developed a post-processing approach to mitigate biases using adversarial examples, uniquely incorporating a GAN-based loss function. Conversely, Zhang et al. employ an architecture similar to ours, generating adversarial perturbations to counteract biases. Our research, however, is distinct in proposing a novel training setup that introduces a unique loss objective along with a curriculum learning strategy. Unlike previous methods that often rely on a single adversarial example, our approach systematically assesses the impact of each adversarial example on the original classifier, providing a fresh perspective.

Curriculum Learning Curriculum learning is an effective training paradigm that gradually exposes models to progressively complex examples, aiding in better generalization [4, 15, 21, 27, 35]. This approach strategically organizes training data, facilitating smoother convergence and improved performance. Several approaches have since been proposed to organize data that include regular sorting of data [4], adaptive organization [35], self-paced curriculum assignment [35], and teacher-based curriculum learning [35].

3 Notations

In our notation, we define the data distribution as D , from which image-label pairs (x, y) are sampled *i.i.d.*, both for train and test data. Protected attribute pairs are denoted as (x_a, y_a) that are again sampled from the same data distribution as (x, y) with adversarial perturbations relative to an attribute-specific image x_a represented by δ_x . The target attribute classifier is $M(\theta, \rho)$, using a backbone network θ and a linear probe ρ , while the protected attribute classifier is $C(\theta, \phi)$, sharing the backbone θ but with a different linear probe ϕ . Predictions from these classifiers are $\hat{Y} = M(\theta, \rho, x)$ for the target and $\bar{Y} = C(\theta, \phi, x_a)$ for the protected attribute.

4 Method

Our method for creating attribute-specific adversarial counterfactuals (ASACs) and employing them to fine-tune a fair model can be broken down into three stages. Initially, we generate ASACs for a set of input images $X = \{x^1, x^2, \dots, x^n\}$,

aiming to mislead the classification model $M(\theta, \rho)$ regarding a protected attribute a (detailed in Section 4.1). For example, when training a smile classifier, we produce adversarial images that prompt misclassification based on the protected attribute of gender. The next step (Section 4.2) evaluates the effectiveness of the generated ASACs. Continuing with our example, we measure the capacity of the ASACs to incorrectly influence the model’s smile classification, even though their primary intent was to confuse the model about gender. We assign a training curriculum based on the ASAC’s success in deceiving the model. This procedure can be seen in Algorithm 1. Finally, the concluding stage utilizes the curriculum and ASACs produced, and introduces an adversarial loss (Section 4.3) to fine-tune the original model $M(\theta, \rho)$. This aims to reduce biases within the model and enhance its discriminative performance.

Algorithm 1 Construct Minibatch for Training based on Curriculum

```

1: function CONSTRUCTCURRICULUM( $M(\theta, \rho)$ ,  $\{x_a(1), \dots, x_a(k)\}$ ,  $\{\epsilon(1), \dots, \epsilon(l)\}$ ,
    $f_{attack}$ , order)
Require:  $M(\theta, \rho)$ : Target attribute classifier
Require:  $\{x_a(1), \dots, x_a(k)\}$ : Attribute-specific minibatch
Require:  $\{\epsilon_1, \dots, \epsilon_l\}$ : Curriculum of noise magnitudes
Require:  $f_{attack}$ : Any scalable adversarial attack
Require: order: Order to sort ASACs in
2:   minibatch  $\leftarrow \{\}$ 
3:   for  $i \leftarrow 1$  to  $k$  do
4:     for  $j \leftarrow 1$  to  $l$  do
5:        $\mathbf{x}'_a \leftarrow f_{attack}(x_a(i), \epsilon_j)$  ▷ Construct ASAC with Eq. 1
6:       score  $\leftarrow DS(\mathbf{x}'_a; M(\theta, \rho))$  ▷ Compute Difficulty Score with Eq. 4
7:       minibatch.append( $\mathbf{x}'_a$ , score)
8:     end for
9:   end for
10:  minibatch.sort( $key = \lambda x : x[1]$ ) ▷ Sort minibatch by difficulty score
11:  return minibatch
12: end function

```

4.1 Generating attribute-specific adversarial examples

This section details our approach to crafting ASACs—adversarial images designed to mislead a model concerning a specific sensitive attribute, denoted as a . We start by employing a target classifier $M(\theta, \rho)$ and develop an attribute classifier, $C(\theta, \phi)$, to predict the protected attribute a within the dataset D . Both models share a similar structure, with only the last layer differing, as depicted in Figure 2. They are trained on identical data distributions D (refer to Section 5.3). To construct each ASAC x_a , we augment the original image x from D with noise δ_{x_a} generated via common methods to generate adversarial images [14, 34]:

$$x_a = x + \delta_{x_a} \quad (1)$$

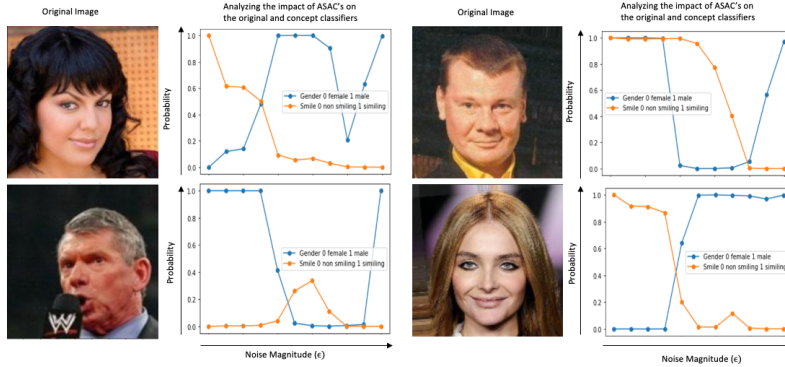


Fig. 3: This figure illustrates the impact of various noise magnitudes on the discriminative power of both the target and protected attribute classifiers for smile and gender, respectively. Our notion of difficulty scores as shown in Equation 4 quantifies the impact that each ASAC has on the original classifier $M(\theta, \phi)$ as shown by the orange data points.

The examples are designed such that outcomes predicted by the models, i.e., $\bar{Y}_a(x'_a)$ and $\bar{Y}_a(x)$ differ while ensuring that the perturbation δ_x is minimal, making the adversarial transformation imperceptible to humans. Examples of such images have been illustrated in Figure 1. As such, these modified examples are crafted to deceive the sensitive attribute classifier, $C(\theta, \phi)$, and not the original model $M(\theta, \phi)$. Given that parameters are shared across both $M(\theta, \rho)$ and $C(\theta, \phi)$, if the outcome to be predicted heavily relies on the protected attribute, a , adversarial examples created to mislead the attribute classifier, $C(\theta, \phi)$, often mislead the predictor $M(\theta, \rho)$ (See Figure 3). Therefore, we refer to them as attribute-specific adversarial counterfactuals.

In our work, we experiment with two commonly used adversarial methods, Fast Gradient Sign Method (FGSM) [14] and Projected Gradient Descent (PGD) [34], to generate images capable of deceiving the attribute classifier. FGSM is a single-step attack approach that perturbs input images based on the gradient sign of the loss function, as shown in Equation 2, with $\epsilon \in [0, 1]$ denoting a scaling factor which we refer to as the noise magnitude.

$$\delta_x = \epsilon \times \text{sign}(\nabla_x J(\theta, \phi, x_a, y_a)) \quad (2)$$

PGD iteratively perturbs input data similar to FGSM to maximize the loss function, aiming to find the smallest perturbation that causes misclassification.

4.2 Curriculum Learning

We propose a curriculum learning based strategy for training our model. Our approach comprises two main stages. Firstly, we evaluate the influence of each ASAC on the classification model $M(\theta, \phi)$ by assessing its difficulty score. Subsequently, the model implements a curriculum for training, guided by the difficulty scores of all examples. By defining a curriculum based on ASACs from different noise magnitudes, we guide the adversarial fine-tuning process, enhancing convergence speed, accuracy, and fairness metrics.

Computing Difficulty Scores The difficulty score plays a key role in curriculum learning as it measures the utility of each example and determines the order in which ASACs are presented to the model during adversarial training [27]. In our problem setting, as in most, it is not feasible to obtain the optimal difficulty score a priori. As such, it is important to come up with a function for measuring the utility of a sample. For any attribute-specific image x_a , we define the difficulty score as the complement of the softmax value the model M returns on x_a :

$$DS(x_a) = 1 - \text{Softmax}(x_a; M_{\theta, \rho}) = 1 - \frac{\exp(M_{\theta, \rho}(x_a))}{\sum_{i=1}^N \exp(M_{\theta, \rho}(x_a(i)))} \quad (3)$$

where N is the number of classes for the target outcome. Note that here we use ASACs for adversarial curriculum learning, therefore, we rewrite Equation (3) as

$$DS(\mathbf{x}'_{\mathbf{a}}) = 1 - \text{Softmax}(\mathbf{x}'_{\mathbf{a}}; M_{\theta, \rho}) \quad (4)$$

A subtle but key point to note here is that the model used to determine the difficulty score and ultimately the curriculum is the target classifier $M(\theta, \rho)$, however, the examples being scored are the ASACs generated, i.e., $\mathbf{x}'_{\mathbf{a}}$ which are generated as a function of the protected attributed classifier $C(\theta, \phi)$. Figure 3 shows the effect of various noise magnitudes on the confidence of the target classifier $M(\theta, \rho)$ in it's prediction. This is analogous to $1 - DS(\mathbf{x}'_{\mathbf{a}})$.

Curriculum Assignment For each minibatch of k attribute-specific images $\{x_a(1), \dots, x_a(k)\}$, we compute the Cartesian product of ASACs with the set of noise l noise magnitudes we use in the curriculum (with $\epsilon = 0$ being one of them). For each of the samples in the resulting minibatch of size $k \times l$, we compute a difficulty score, $DS(\mathbf{x}'_{\mathbf{a}})$, detailed in Equation 4, that scores an ASAC based on the hardness of the example for the target classifier. We then sort the minibatch based on the hardness of each sample. See Table 3 for an ablation on the effect of a randomized, increasing, and decreasing order (*w.r.t.* difficulty score) for samples in the curriculum. This procedure is illustrated in detail in Algorithm 1 and enables what defines each in-batch curriculum for corresponding minibatches in the fine-tuning process for the target attribute classifier $M(\theta, \rho)$.

4.3 Fine-Grained Control using Adversarial Loss

It is important to note that in **all** curriculums experimented with, we include the original minibatch, i.e., $\epsilon = 0$. When performing any kind of adversarial training, there exists the possibility of overfitting, especially when fine-tuning a model over the same or similar data it was originally trained on. Though overfitting may lead to improved fairness metrics, it results in a lower degree of generalization of the model. While fine-tuning the target classifier $M(\theta, \rho)$, we use *Cross Entropy* (CE) as our loss function (J); however, any fully differentiable loss function may be used. We extend our approach to address the issue of overfitting and the ability to have fine-grained control over the trade-off between accuracy and fairness by introducing an adversarial regularization term, α . We construct our loss function \hat{J} to contain two terms, both governed by a convex combination of α as shown in the equation below:

$$\hat{J}_\alpha(\theta, \rho, x_a; \mathbf{x}'_a, y) = \alpha J(\theta, \rho, x_a, y) + (1 - \alpha) J(\theta, \rho, \mathbf{x}'_a, y) \quad (5)$$

Increasing values of α increases the attention the model pays to the unperturbed images x_a , while decreasing values of α increases the attention the model pays to the ASACs produced, allowing for more fine-grained control of the model produced during the fine-tuning procedure. This enables adopters of the method to fine-tune models based on their specific needs.

5 Experiment Setup

This section describes our experimental setup. We outline the datasets used, followed by the evaluation metrics that are employed to evaluate the model and finally describe the training details.

5.1 Datasets

Similar to Wang et al.’s approach [58], we use the CelebA [31] and LFW [19] datasets. CelebA contains 202,599 images annotated with 40 attributes and we focus on Smiling, Big Nose, and Wavy Hair, with Gender as the protected attribute. Similarly, LFW comprises 13,244 images annotated with 73 attributes, where we select Smile, Wavy Hair, and Bags Under Eyes, with Gender as the protected attribute.

5.2 Evaluation Metrics

To evaluate the fairness of our model, we employ three key metrics: the Difference in Demographic Parity (DDP), the Difference in Equalized Odds (DEO), and the Difference in Equalized Opportunity (DEOp) [16]. Alongside these, we also measure the model’s accuracy (ACC). Lower values for fairness metrics indicate a less biased model whereas a high value in accuracy indicates a more performant model. For more details about the metrics and their definition please refer to the supplementary material (Sections ?? and ??).

Table 1: Performance across accuracy and fairness metrics on the CelebA dataset. Note that the fairness metrics for the proposed approach with PGD for a Big Nose classifier are not calculated as the model assigned the same label to all examples.

| Label | Method | DEO | DEO _q | DDP | ACC |
|-----------|-------------------------------|--------------|------------------|--------------|--------------|
| Smile | Base Classifier | 0.088 | 0.066 | 0.15 | 84.29 |
| | Zhang and Sang [63] | 0.077 | 0.051 | 0.17 | 91.74 |
| | Proposed Approach (with FGSM) | 0.050 | 0.043 | 0.15 | 91.79 |
| | Proposed Approach (with PGD) | 0.058 | 0.045 | 0.14 | 91.20 |
| Big Nose | Base Classifier | 0.332 | 0.257 | 0.283 | 80.77 |
| | Zhang and Sang [63] | 0.396 | 0.311 | 0.355 | 81.53 |
| | Proposed Approach (with FGSM) | 0.354 | 0.267 | 0.306 | 82.05 |
| | Proposed Approach (with PGD) | - | - | - | 78.80 |
| Wavy Hair | Base Classifier | 0.347 | 0.237 | 0.347 | 81.15 |
| | Zhang and Sang [63] | 0.359 | 0.264 | 0.396 | 82.07 |
| | Proposed Approach (with FGSM) | 0.344 | 0.228 | 0.342 | 82.01 |
| | Proposed Approach (with PGD) | 0.383 | 0.243 | 0.341 | 81.99 |

5.3 Training Details

We utilize ResNet-18 [17] as the backbone architecture, pretrained for 50 epochs and fine-tuned with our proposed approach for 10 epochs, utilizing the same data distribution D . A batch size of 128 is used with Adam optimizer (learning rate 10^{-4}). We experiment with $\epsilon \in [0, 1]$ for varying adversarial noise levels in images, with smaller ϵ implying less noise and values closer to 1 indicating higher corruption.

6 Results

In this section, we present and discuss various experiments to evaluate and interpret our proposed approach. We evaluate our approach through quantitative performance metrics and fairness evaluations, followed by qualitative analysis using interpretability methods. We also conduct ablations on curriculum policies, noise magnitudes (ϵ), and adversarial loss weights (α).

6.1 Quantitative Results

Table 1 presents quantitative results for models trained with and without our proposed approach on the CelebA dataset [31]. We perform our analysis on the target attributes of Smiling, Big Nose, and Wavy Hair. We consider the protected attribute in all cases to be Gender. We compare the proposed approach (utilizing both FGSM [14] and PGD [34] adversarial methods) with two other strategies: the original baseline model, a similar previous approach employing adversarial

Table 2: Performance across accuracy and fairness metrics on the LFW dataset.

| Label | Method | DEO | DEOq | DDP | ACC |
|-----------------|-------------------------------|--------------|--------------|-------------|--------------|
| Smile | Base Classifier | 0.074 | 0.071 | 0.19 | 71.29 |
| | Zhang and Sang [63] | 0.065 | 0.059 | 0.18 | 84.74 |
| | Proposed Approach (with FGSM) | 0.054 | 0.050 | 0.16 | 89.19 |
| | Proposed Approach (with PGD) | 0.063 | 0.060 | 0.16 | 88.41 |
| Bags Under Eyes | Base Classifier | 0.074 | 0.073 | 0.16 | 69.29 |
| | Zhang and Sang [63] | 0.064 | 0.061 | 0.14 | 74.27 |
| | Proposed Approach (with FGSM) | 0.061 | 0.060 | 0.14 | 87.29 |
| | Proposed Approach (with PGD) | 0.066 | 0.062 | 0.17 | 86.42 |
| Wavy Hair | Base Classifier | 0.082 | 0.072 | 0.18 | 63.29 |
| | Zhang and Sang [63] | 0.065 | 0.064 | 0.19 | 73.27 |
| | Proposed Approach (with FGSM) | 0.066 | 0.062 | 0.19 | 88.29 |
| | Proposed Approach (with PGD) | 0.065 | 0.067 | 0.16 | 88.70 |

training strategies [63]. Our proposed approach not only enhances the overall accuracy of all the target classifiers (we observe the trend for Smile and Wavy Hair however, the fairness metrics increase for Big Nose) but also demonstrates improvements across all fairness metrics evaluated.

We conduct the same analysis on the LFW dataset [19], targeting attributes such as Smiling, Bags Under Eyes, and Wavy Hair, considering the influence of Gender as the protected attribute. The results are summarized in Table 2. Our findings on our proposed approach on the LFW dataset [19] are consistent with those on the CelebA dataset [31], indicating an increase in overall accuracy and improvements across most fairness metrics (we observe the trend for all the three classifiers Smile, Bags Under Eyes and Wavy Hair).

6.2 Qualitative Results

Robustness evaluation of adversarial training To assess the impact of adversarial training using ASACs, we examine how adversarial images designed to attack a gender classifier affects the decision of the smile classifier, pre and post-training with our proposed approach. Given an image, we add varying magnitudes of adversarial noise and provide the corrupted images to the smile classifier. We observe that before using our proposed method, the noise intended to mislead the gender classifier also misled the smile classifier, indicating a strong correlation between gender and smile attributes in these examples. Such an outcome suggests that manipulations that target gender can inadvertently influence predictions on smile. We perform an identical analysis on the models after our proposed fine-tuning approach. Some of these examples have been demonstrated in Figure 4, we observe that after fine-tuning the smile classifier with our proposed approach, on these examples the model improves in its discriminative ability, and while the gender classifier is still confused about these examples,

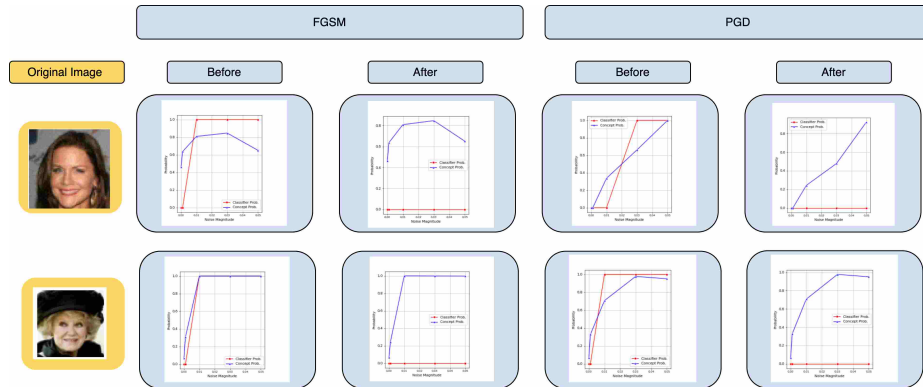


Fig. 4: A comparison of the confidence of the smile classifier in its prediction, in response to ASACs constructed at various noise magnitudes. The response is measured before (in blue) and after (in red) the proposed fine-tuning procedure. We observe more consistency in the model’s ability to maintain its prediction, indicating a resilience to ASAC-induced decision flips.

our model does not get confused by ASACs. Our findings indicate that the fine-tuning procedure effectively might be able to decouple the smile classifier from spurious correlations with gender, thus bolstering its ability to independently make precise predictions.

Integrated Gradients To assess the impact of ASAC-driven adversarial and curriculum-based fine-tuning, we observe the effect our approach has on individual samples in the test set using Integrated Gradients (IG) [49]. Integrated Gradients is a widely recognized interpretability technique that highlights the pixels influencing decision-making process of the model. In Figure 5, we juxtapose the integrated gradients of decisions made by the classifier both pre and post ASAC training. For more examples, see supplementary section 8.3.

After applying our proposed approach, the integrated gradients converge towards the mouth area in the images. As humans, we can agree that the mouth area is the largest indicator of whether a person is smiling or not. Our observations suggest that ASAC-driven training compels the model to focus on regions of the image more closely correlated with a smile. Consequently, these findings indicate that the model fine-tuned using ASACs may give more importance to regions closer to the mouth compared to earlier model.

t-SNE We utilize t-SNE [33], a method for visualizing high-dimensional data in a lower-dimensional space, to illustrate the efficacy of our method in disentangling sensitive information within the vision space. Specifically, we aim to demonstrate that our approach can strategically map images closer to the protected attribute decision hyperplane while preserving their distance from the target label decision hyperplane in the latent space of the deployed model. To visualize this, we extract feature vectors for images passed through the models

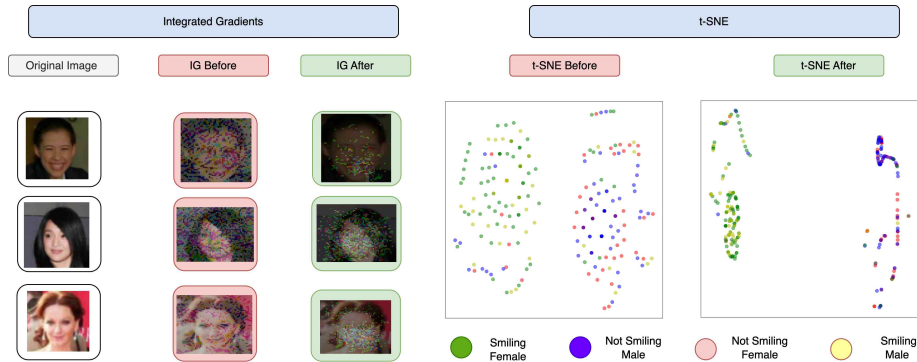


Fig. 5: We look at the Integrated Gradients (left) and t-SNE curves (right) for samples before and after training.

Table 3: A comparison of different curriculum learning strategies.

| Method | DEO | DEOq | DDP | ACC |
|---|--------------|--------------|-------------|--------------|
| W/O Curriculum Learning | 0.055 | 0.044 | 0.14 | 91.23 |
| Curriculum Learning in Ascending order | 0.050 | 0.043 | 0.15 | 91.79 |
| Curriculum Learning in Descending order | 0.058 | 0.048 | 0.17 | 92.08 |

before and after applying our approach. We then use t-SNE to plot them in a two-dimensional space (Figure 5). This comparison shows our approach’s effectiveness in improving model separability. As shown in the figure, after training samples are more distinguishable, suggesting that our method hides sensitive information while preserving essential characteristics for accurate classification.

6.3 Ablation Study

Evaluating the impact of Curriculum Learning In our ablation analyses, we test different training strategies: one based on curriculum learning, where difficulty increases gradually, and another where the model faces the toughest examples first. Results (see Table 3) show that while starting with challenging examples boosts accuracy, saving them for later enhances fairness metrics. This underscores the importance of curriculum design in balancing accuracy and fairness in machine learning models. The study highlights the role of curriculum design in shaping the trade-off between accuracy and fairness in our approach.

Finding the most optimal noise magnitudes In our second ablation study (Table 4), we investigate the effect of varying noise magnitudes on our smile classifier model’s performance. Using FGSM as our chosen adversarial image generation method, we test different magnitudes of ϵ before implementing curriculum learning. Our results show that $\epsilon = 0.03$ and $\epsilon = 0.05$ yield optimal performance. We then incorporate examples generated at these magnitudes, along

Table 4: Ablation on the effect of different values of ϵ and α on the performance and fairness metrics of the target classifier utilizing FGSM for ASAC generation.

| Parameter | Setting | DEO | DEOq | DDP | ACC |
|------------|-------------------|-------|-------|------|-------|
| ϵ | {0.001,0.03,0.05} | 0.065 | 0.047 | 0.16 | 91.00 |
| | {0.001} | 0.054 | 0.043 | 0.14 | 91.62 |
| | {0.05} | 0.055 | 0.044 | 0.14 | 91.71 |
| | {0.001,0.03,0.05} | 0.057 | 0.048 | 0.16 | 91.73 |
| | {0.001,0.03} | 0.055 | 0.043 | 0.14 | 91.42 |
| | {0.001,0.05} | 0.057 | 0.047 | 0.14 | 91.38 |
| α | 0.3 | 0.06 | 0.04 | 0.16 | 92.04 |
| | 0.5 | 0.058 | 0.050 | 0.16 | 91.84 |
| | 0.7 | 0.057 | 0.047 | 0.14 | 91.90 |

with original images, into our curriculum learning setup. This experimentation offers valuable insights into selecting noise magnitudes that enhance the model’s robustness and effectiveness in adversarial scenarios.

Choosing an Optimal α In our third ablation study (Table 4), we examine the impact of different α values (0.3, 0.5, and 0.7) on model performance. Lower α (0.3) leads to higher accuracy, whereas $\alpha = 0.5$ prioritizes fairness metrics. We select $\alpha = 0.5$ for final model training, emphasizing the importance of balancing accuracy and fairness. Though a lower value of α boosts accuracy, $\alpha = 0.5$ achieves favorable fairness outcomes, ensuring a more equitable model.

7 Conclusion

We propose a method for utilizing attribute-specific adversarial examples as counterfactuals to enhance fairness in computer vision models. Our method fine-tunes models with these counterfactuals using a novel curriculum learning training regime. Our experiments on CelebA and LFW datasets demonstrate that adversarial fine-tuning significantly improves fairness metrics without sacrificing accuracy, with no discernible fairness-accuracy tradeoff. Qualitative results indicate the model’s ability to disentangle decisions from protected attributes. Ablation studies justify different design choices, notably revealing that starting with challenging examples may lead to a more accurate model, while presenting easier examples earlier results in a fairer but less accurate model. This underscores the impact of curriculum learning on the problem.

Ethical Considerations. Our work targets the ethical concerns surrounding biases in computer vision models. Further, our approach can be used to mitigate biases by fine-tuning existing biased models and can also be deployed in a low-data setting. The main limitation of our work is that it requires the backbone of our model and cannot be applied on a black-box model.

References

1. Abbasnejad, E., Teney, D., Parvaneh, A., Shi, J., Hengel, A.v.d.: Counterfactual vision and language learning. In: Proceedings of the IEEE/CVF conference on computer vision and pattern recognition. pp. 10044–10054 (2020)
2. Abid, A., Yuksekgonul, M., Zou, J.: Meaningfully debugging model mistakes using conceptual counterfactual explanations. In: International Conference on Machine Learning. pp. 66–88. PMLR (2022)
3. Balakrishnan, G., Xiong, Y., Xia, W., Perona, P.: Towards causal benchmarking of bias in face analysis algorithms. In: Deep Learning-Based Face Analytics, pp. 327–359. Springer (2021)
4. Bengio, Y., Louradour, J., Collobert, R., Weston, J.: Curriculum learning. In: Proceedings of the 26th annual international conference on machine learning. pp. 41–48 (2009)
5. Beutel, A., Chen, J., Zhao, Z., Chi, E.H.: Data decisions and theoretical implications when adversarially learning fair representations. arXiv preprint arXiv:1707.00075 (2017)
6. Bolukbasi, T., Chang, K.W., Zou, J.Y., Saligrama, V., Kalai, A.T.: Man is to computer programmer as woman is to homemaker? debiasing word embeddings. *Advances in neural information processing systems* **29** (2016)
7. Buolamwini, J., Gebru, T.: Gender shades: Intersectional accuracy disparities in commercial gender classification. In: Conference on fairness, accountability and transparency. pp. 77–91. PMLR (2018)
8. Chen, Z., Gao, Q., Bosselut, A., Sabharwal, A., Richardson, K.: Disco: distilling counterfactuals with large language models. In: Proceedings of the 61st Annual Meeting of the Association for Computational Linguistics (Volume 1: Long Papers). pp. 5514–5528 (2023)
9. Cheong, J., Kalkan, S., Gunes, H.: Counterfactual fairness for facial expression recognition. In: European Conference on Computer Vision. pp. 245–261. Springer (2022)
10. Chinchure, A., Shukla, P., Bhatt, G., Salij, K., Hosanagar, K., Sigal, L., Turk, M.: Tibet: Identifying and evaluating biases in text-to-image generative models. arXiv preprint arXiv:2312.01261 (2023)
11. Dash, S., Balasubramanian, V.N., Sharma, A.: Evaluating and mitigating bias in image classifiers: A causal perspective using counterfactuals. In: Proceedings of the IEEE/CVF Winter Conference on Applications of Computer Vision. pp. 915–924 (2022)
12. Denton, E., Hutchinson, B., Mitchell, M., Gebru, T., Zaldivar, A.: Image counterfactual sensitivity analysis for detecting unintended bias. arXiv preprint arXiv:1906.06439 (2019)
13. Feder, A., Oved, N., Shalit, U., Reichart, R.: Causalm: Causal model explanation through counterfactual language models. *Computational Linguistics* **47**(2), 333–386 (2021)
14. Goodfellow, I.J., Shlens, J., Szegedy, C.: Explaining and harnessing adversarial examples. arXiv preprint arXiv:1412.6572 (2014)
15. Graves, A., Bellemare, M.G., Menick, J., Munos, R., Kavukcuoglu, K.: Automated curriculum learning for neural networks. In: international conference on machine learning. pp. 1311–1320. Pmlr (2017)
16. Hardt, M., Price, E., Srebro, N.: Equality of opportunity in supervised learning. *Advances in neural information processing systems* **29** (2016)

17. He, K., Zhang, X., Ren, S., Sun, J.: Deep residual learning for image recognition. In: Proceedings of the IEEE conference on computer vision and pattern recognition. pp. 770–778 (2016)
18. Hendricks, L.A., Burns, K., Saenko, K., Darrell, T., Rohrbach, A.: Women also snowboard: Overcoming bias in captioning models. In: Proceedings of the European conference on computer vision (ECCV). pp. 771–787 (2018)
19. Huang, G.B., Ramesh, M., Berg, T., Learned-Miller, E.: Labeled faces in the wild: A database for studying face recognition in unconstrained environments. Tech. Rep. 07-49, University of Massachusetts, Amherst (October 2007)
20. Jiang, L., Ma, X., Chen, S., Bailey, J., Jiang, Y.G.: Black-box adversarial attacks on video recognition models. In: Proceedings of the 27th ACM International Conference on Multimedia. pp. 864–872 (2019)
21. Jiang, L., Meng, D., Zhao, Q., Shan, S., Hauptmann, A.: Self-paced curriculum learning. In: Proceedings of the AAAI Conference on Artificial Intelligence. vol. 29 (2015)
22. Joshi, A.R., Cuadros, X.S., Sivakumar, N., Zappella, L., Apostoloff, N.: Fair sa: Sensitivity analysis for fairness in face recognition. In: Algorithmic fairness through the lens of causality and robustness workshop. pp. 40–58. PMLR (2022)
23. Karimi, A.H., Barthe, G., Balle, B., Valera, I.: Model-agnostic counterfactual explanations for consequential decisions. In: International Conference on Artificial Intelligence and Statistics. pp. 895–905. PMLR (2020)
24. Karras, T., Laine, S., Aittala, M., Hellsten, J., Lehtinen, J., Aila, T.: Analyzing and improving the image quality of stylegan. In: Proceedings of the IEEE/CVF conference on computer vision and pattern recognition. pp. 8110–8119 (2020)
25. Kasirzadeh, A., Smart, A.: The use and misuse of counterfactuals in ethical machine learning. In: Proceedings of the 2021 ACM Conference on Fairness, Accountability, and Transparency. pp. 228–236 (2021)
26. Kaushik, D., Hovy, E., Lipton, Z.C.: Learning the difference that makes a difference with counterfactually-augmented data. arXiv preprint arXiv:1909.12434 (2019)
27. Kong, Y., Liu, L., Wang, J., Tao, D.: Adaptive curriculum learning. In: Proceedings of the IEEE/CVF International Conference on Computer Vision. pp. 5067–5076 (2021)
28. Kusner, M.J., Loftus, J., Russell, C., Silva, R.: Counterfactual fairness. *Advances in neural information processing systems* **30** (2017)
29. Lim, J., Kim, Y., Kim, B., Ahn, C., Shin, J., Yang, E., Han, S.: Biasadv: Bias-adversarial augmentation for model debiasing. In: Proceedings of the IEEE/CVF Conference on Computer Vision and Pattern Recognition. pp. 3832–3841 (2023)
30. Liu, B., Deng, W., Zhong, Y., Wang, M., Hu, J., Tao, X., Huang, Y.: Fair loss: Margin-aware reinforcement learning for deep face recognition. In: Proceedings of the IEEE/CVF international conference on computer vision. pp. 10052–10061 (2019)
31. Liu, Z., Luo, P., Wang, X., Tang, X.: Deep learning face attributes in the wild. In: Proceedings of International Conference on Computer Vision (ICCV) (December 2015)
32. Lohia, P.K., Ramamurthy, K.N., Bhide, M., Saha, D., Varshney, K.R., Puri, R.: Bias mitigation post-processing for individual and group fairness. In: *Icassp 2019-2019 IEEE international conference on acoustics, speech and signal processing (icassp)*. pp. 2847–2851. IEEE (2019)
33. Van der Maaten, L., Hinton, G.: Visualizing data using t-sne. *Journal of machine learning research* **9**(11) (2008)

34. Madry, A., Makelov, A., Schmidt, L., Tsipras, D., Vladu, A.: Towards deep learning models resistant to adversarial attacks. arXiv preprint arXiv:1706.06083 (2017)
35. Matiisen, T., Oliver, A., Cohen, T., Schulman, J.: Teacher–student curriculum learning. *IEEE transactions on neural networks and learning systems* **31**(9), 3732–3740 (2019)
36. Maudslay, R.H., Gonen, H., Cotterell, R., Teufel, S.: It’s all in the name: Mitigating gender bias with name-based counterfactual data substitution. In: Inui, K., Jiang, J., Ng, V., Wan, X. (eds.) *Proceedings of the 2019 Conference on Empirical Methods in Natural Language Processing and the 9th International Joint Conference on Natural Language Processing (EMNLP-IJCNLP)*. pp. 5267–5275. Association for Computational Linguistics, Hong Kong, China (Nov 2019). <https://doi.org/10.18653/v1/D19-1530>, <https://aclanthology.org/D19-1530>
37. Meister, N., Zhao, D., Wang, A., Ramaswamy, V.V., Fong, R., Russakovsky, O.: Gender artifacts in visual datasets. In: *Proceedings of the IEEE/CVF International Conference on Computer Vision*. pp. 4837–4848 (2023)
38. Mothilal, R.K., Sharma, A., Tan, C.: Explaining machine learning classifiers through diverse counterfactual explanations. In: *Proceedings of the 2020 conference on fairness, accountability, and transparency*. pp. 607–617 (2020)
39. Narodytska, N., Kasiviswanathan, S.: Simple black-box adversarial attacks on deep neural networks. In: *2017 IEEE Conference on Computer Vision and Pattern Recognition Workshops (CVPRW)*. pp. 1310–1318 (2017). <https://doi.org/10.1109/CVPRW.2017.172>
40. Pawelczyk, M., Agarwal, C., Joshi, S., Upadhyay, S., Lakkaraju, H.: Exploring counterfactual explanations through the lens of adversarial examples: A theoretical and empirical analysis. In: *International Conference on Artificial Intelligence and Statistics*. pp. 4574–4594. PMLR (2022)
41. Qiu, H., Xiao, C., Yang, L., Yan, X., Lee, H., Li, B.: Semanticadv: Generating adversarial examples via attribute-conditioned image editing. In: *Computer Vision–ECCV 2020: 16th European Conference, Glasgow, UK, August 23–28, 2020, Proceedings, Part XIV 16*. pp. 19–37. Springer (2020)
42. Quadrianto, N., Sharmanska, V., Thomas, O.: Discovering fair representations in the data domain. In: *Proceedings of the IEEE/CVF conference on computer vision and pattern recognition*. pp. 8227–8236 (2019)
43. Rahmati, A., Moosavi-Dezfooli, S.M., Frossard, P., Dai, H.: Geoda: a geometric framework for black-box adversarial attacks. In: *Proceedings of the IEEE/CVF conference on computer vision and pattern recognition*. pp. 8446–8455 (2020)
44. Ramaswamy, V.V., Kim, S.S., Russakovsky, O.: Fair attribute classification through latent space de-biasing. In: *Proceedings of the IEEE/CVF conference on computer vision and pattern recognition*. pp. 9301–9310 (2021)
45. Roh, Y., Lee, K., Whang, S., Suh, C.: Fr-train: A mutual information-based approach to fair and robust training. In: *International Conference on Machine Learning*. pp. 8147–8157. PMLR (2020)
46. Seyyed-Kalantari, L., Zhang, H., McDermott, M.B., Chen, I.Y., Ghassemi, M.: Underdiagnosis bias of artificial intelligence algorithms applied to chest radiographs in under-served patient populations. *Nature medicine* **27**(12), 2176–2182 (2021)
47. Shi, Y., Yu, X., Sohn, K., Chandraker, M., Jain, A.K.: Towards universal representation learning for deep face recognition. In: *Proceedings of the IEEE/CVF Conference on Computer Vision and Pattern Recognition*. pp. 6817–6826 (2020)
48. Sokol, K., Flach, P.A.: Counterfactual explanations of machine learning predictions: Opportunities and challenges for ai safety. *SafeAI@ AAAI* pp. 1–4 (2019)

49. Sundararajan, M., Taly, A., Yan, Q.: Axiomatic attribution for deep networks. In: International conference on machine learning. pp. 3319–3328. PMLR (2017)
50. Szegedy, C., Zaremba, W., Sutskever, I., Bruna, J., Erhan, D., Goodfellow, I., Fergus, R.: Intriguing properties of neural networks. arXiv preprint arXiv:1312.6199 (2013)
51. Ustun, B., Spangher, A., Liu, Y.: Actionable recourse in linear classification. In: Proceedings of the conference on fairness, accountability, and transparency. pp. 10–19 (2019)
52. Van Looveren, A., Klaise, J.: Interpretable counterfactual explanations guided by prototypes. In: Joint European Conference on Machine Learning and Knowledge Discovery in Databases. pp. 650–665. Springer (2021)
53. Vandenhende, S., Mahajan, D., Radenovic, F., Ghadiyaram, D.: Making heads or tails: Towards semantically consistent visual counterfactuals. In: European Conference on Computer Vision. pp. 261–279. Springer (2022)
54. Wang, A., Liu, A., Zhang, R., Kleiman, A., Kim, L., Zhao, D., Shirai, I., Narayanan, A., Russakovsky, O.: Revise: A tool for measuring and mitigating bias in visual datasets. *International Journal of Computer Vision* **130**(7), 1790–1810 (2022)
55. Wang, A., Russakovsky, O.: Overwriting pretrained bias with finetuning data. In: Proceedings of the IEEE/CVF International Conference on Computer Vision. pp. 3957–3968 (2023)
56. Wang, H., Wang, Z., Du, M., Yang, F., Zhang, Z., Ding, S., Mardziel, P., Hu, X.: Score-cam: Score-weighted visual explanations for convolutional neural networks. In: Proceedings of the IEEE/CVF conference on computer vision and pattern recognition workshops. pp. 24–25 (2020)
57. Wang, J.: Adversarial examples in physical world. In: IJCAI. pp. 4925–4926 (2021)
58. Wang, J., Liu, Y., Wang, X.: Assessing multilingual fairness in pre-trained multimodal representations. In: Findings of the Association for Computational Linguistics: ACL 2022. pp. 2681–2695 (2022)
59. Wang, Z., Qinami, K., Karakozis, I.C., Genova, K., Nair, P., Hata, K., Russakovsky, O.: Towards fairness in visual recognition: Effective strategies for bias mitigation. In: Proceedings of the IEEE/CVF conference on computer vision and pattern recognition. pp. 8919–8928 (2020)
60. Wang, Z., Dong, X., Xue, H., Zhang, Z., Chiu, W., Wei, T., Ren, K.: Fairness-aware adversarial perturbation towards bias mitigation for deployed deep models. In: Proceedings of the IEEE/CVF Conference on Computer Vision and Pattern Recognition. pp. 10379–10388 (2022)
61. Wu, T., Ribeiro, M.T., Heer, J., Weld, D.S.: Polyjuice: Generating counterfactuals for explaining, evaluating, and improving models. In: Proceedings of the 59th Annual Meeting of the Association for Computational Linguistics and the 11th International Joint Conference on Natural Language Processing (Volume 1: Long Papers). pp. 6707–6723 (2021)
62. Zeng, P., Li, Y., Hu, P., Peng, D., Lv, J., Peng, X.: Deep fair clustering via maximizing and minimizing mutual information: Theory, algorithm and metric. In: Proceedings of the IEEE/CVF Conference on Computer Vision and Pattern Recognition. pp. 23986–23995 (2023)
63. Zhang, Y., Sang, J.: Towards accuracy-fairness paradox: Adversarial example-based data augmentation for visual debiasing. In: Proceedings of the 28th ACM International Conference on Multimedia. pp. 4346–4354 (2020)

8 Supplementary Material

8.1 Fairness Definitions

To evaluate the fairness of our model, we employ three key metrics: the Difference in Demographic Parity (DDP), the Difference in Equalized Odds (DEO), and the Difference in Equalized Opportunity (DEOp). Alongside these, we also measure the model’s accuracy (ACC).

The DEO focuses on the difference in the rates of false negatives and false positives between genders. A substantial DEO indicates a bias in which one group is either less likely to be incorrectly dismissed or more likely to be inaccurately favored.

Definition 1 (Equalized Odds). *A predictor \hat{Y} satisfies equalized odds with respect to protected attribute $A \in \{a, a'\}$ and outcome Y , if \hat{Y} and A are independent conditional on Y .*

$$P(\hat{Y} = 1|Y = y, A = a) = P(\hat{Y} = 1|Y = y, A = a') \quad \text{where } y \in \{0, 1\}. \quad (6)$$

To estimate how far a predictor \hat{Y} from having equalized odds, we estimate the Difference in Equalized Odds (DEO), i.e., we estimate

$$\frac{\sum_{y \in \{0, 1\}} |P(\hat{Y} = 1|Y = y, A = a) - P(\hat{Y} = 1|Y = y, A = a')|}{2}.$$

DDP quantifies the absolute gap in approval rates (e.g., smile prediction) across different protected attributes. A large DDP value suggests a tendency for individuals in a specific group to receive more favorable outcomes than their counterparts in the other group.

Definition 2 (Demographic Parity). *A predictor \hat{Y} satisfies demographic parity with respect to protected attribute $A \in \{a, a'\}$ and outcome Y , if the following condition holds:*

$$P(\hat{Y} = 1|A = a) = P(\hat{Y} = 1|A = a'). \quad (7)$$

To estimate how far a predictor \hat{Y} from having demographic parity, we estimate the Difference in Demographic Parity (DDP), i.e., we estimate

$$|P(\hat{Y} = 1|A = a) - P(\hat{Y} = 1|A = a')|.$$

The Difference in Equalized Opportunity (DEOp) measures the disparity in True Positive Rates between different demographic groups in a model, indicating bias in favorable outcomes. A DEOp of zero signifies equal accuracy across groups, representing a fairness ideal in model performance. The difference in Equalized Opportunity is given as follows.

Definition 3 (Equalized Opportunity). A predictor \hat{Y} satisfies equalized opportunity with respect to protected attribute $A \in \{a, a'\}$ and outcome Y , if the following condition holds for a specific outcome value y :

$$P(\hat{Y} = 1|Y = 1, A = a) = P(\hat{Y} = 1|Y = 1, A = a').$$

To measure how far a predictor \hat{Y} from having demographic parity, we estimate the Difference in Equalized Opportunity (DEOp), i.e., we estimate

$$|P(\hat{Y} = 1|Y = 1, A = a) - P(\hat{Y} = 1|Y = 1, A = a')|.$$

Ideally, we want these values to be zero, indicating no disparity.

8.2 Additional Robustness Results

This section shows some additional positive (Figure 6) and negative results (Figure 7) similar to the qualitative results shown in Section 6.2. It should be noted that however, some samples are not impacted by adding adversarial noise and as a result, the values of the smile classifier do not change. These examples have been shown in Figure 7.

8.3 Additional IG Results

In Figure 8, we show more examples of how Integrated Gradients (IG) change on sample pictures after we use our new method. Integrated Gradients help us see which parts of the picture affect the model’s decisions the most. We did our tests the same way we explained in Section 6.2. Examples presented in Figure 8 show a similar trend to Figure 5 and the pixels that are used in decision-making converge from the entire towards the mouth region after applying our approach.



Fig. 6: Qualitative results showing that our trained model becomes robust to ASACs after training.



Fig. 7: Examples where the adversarial noise is unable to flip the smile classifier. As shown in the figure adding adversarial noise does not change the decision of the smile classifier (red curve). Post training, the decision remains unchanged as well.

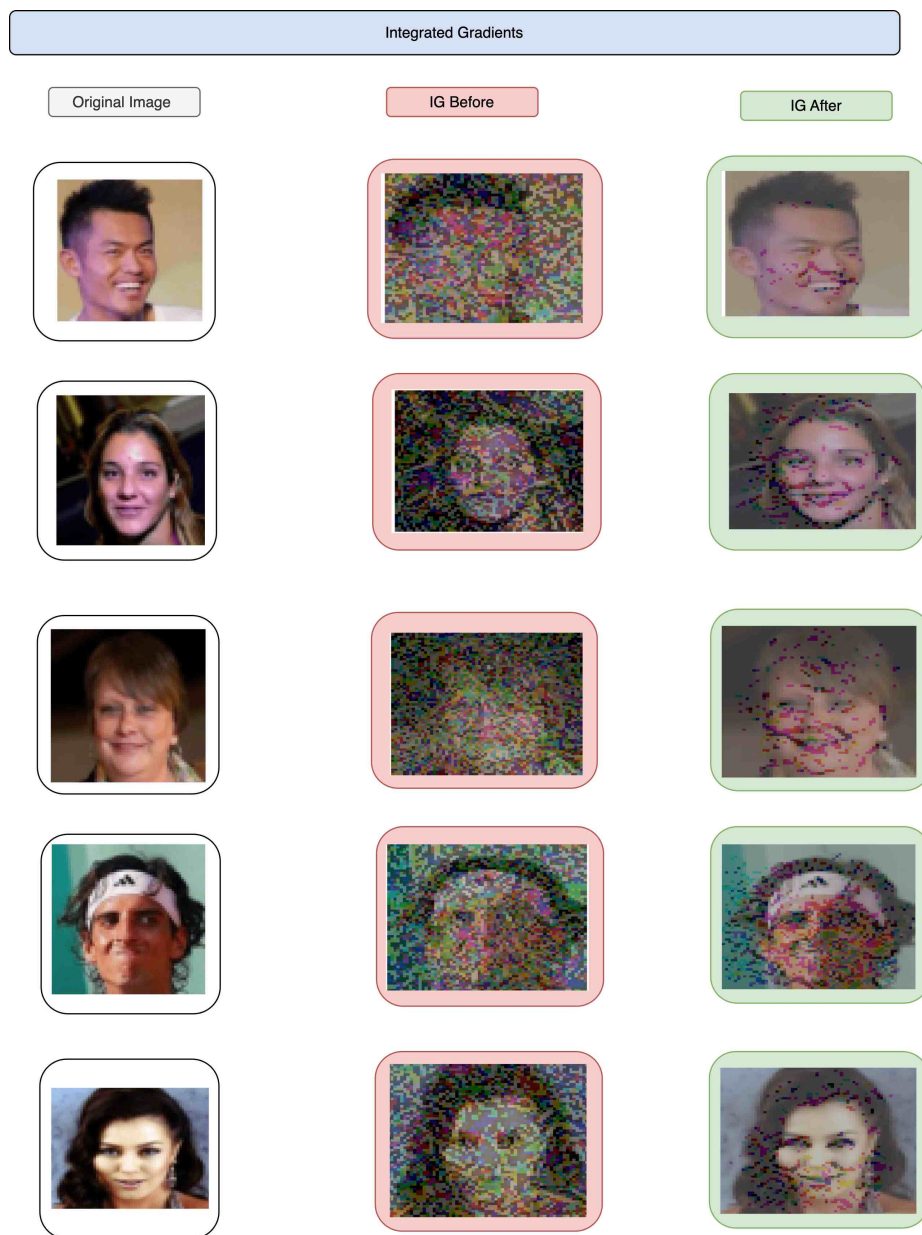


Fig. 8: More examples showcasing the change in integrated gradients for the smile classifier before and after applying our method.